Chapter 12

Synchronization Phenomena in Coupled Birkhoff-Shaw Chaotic Systems Using Nonlinear Controllers

Christos K. Volos, Hector E. Nistazakis,
Ioannis M. Kyprianidis, Ioannis N. Stouboulos and
George S. Tombras

Additional information is available at the end of the chapter

http://dx.doi.org/10.5772/64811

Abstract

In this chapter, the well-known non-autonomous chaotic system, the Birkhoff-Shaw, which exhibits the structure of beaks and wings, typically observed in chaotic neuronal models, is used in a coupling scheme. The Birkhoff-Shaw system is a second-order non-autonomous dynamical system with rich dynamical behaviour, which has not been sufficiently studied. Furthermore, the master-slave (unidirectional) coupling scheme, which is used, is designed by using the nonlinear controllers to target synchronization states, such as complete synchronization and antisynchronization, with amplification or attenuation in chaotic oscillators. It is the first time that the specific method has been used in coupled non-autonomous chaotic systems. The stability of synchronization is ensured by using Lyapunov function stability theorem in the unidirectional mode of coupling. The simulation results from system's numerical integration confirm the appearance of complete synchronization and antisynchronization phenomena depending on the signs of the parameters of the error functions. Electronic circuitry that models the coupling scheme is also reported to verify its feasibility.

Keywords: chaos, complete synchronization, antisynchronization, anidirectional coupling, nonlinear controller

1. Introduction

In the past decades, the phenomenon of synchronization between coupled nonlinear systems and especially of systems with chaotic behaviour has attracted scientists' interest from all over

the world because it is an interesting phenomenon with a broad range of applications, such as in various complex physical, chemical and biological systems [1–9], in secure and broadband communication system [10, 11] and in cryptography [12, 13].

In synchronization two or more systems with chaotic behaviour can adjust a given of their motion property to a common behaviour (equal trajectories or phase locking), due to forcing or coupling [14]. However, having two chaotic systems being synchronized, it is a major surprise, due to the exponential divergence of the nearby trajectories of the systems. Nevertheless, nowadays the phenomenon of synchronization of coupled chaotic oscillators is well-studied theoretically and proven experimentally.

Synchronization theory has begun studying in the 1980s and early 1990s by Fujisaka and Yamada [15], Pikovsky [16], Pecora and Carroll [17]. Onwards, a great number of research works based on synchronization of nonlinear systems has risen and many synchronization schemes depending on the nature of the coupling schemes and of the interacting systems have been presented. Complete or full chaotic synchronization [18–23], phase synchronization [24, 25], lag synchronization [26, 27], generalized synchronization [28], antisynchronization [29, 30], anti-phase synchronization [31–36], projective synchronization [37], anticipating [38] and inverse lag synchronization [39] are the most interesting types of synchronization, which have been investigated numerically and experimentally by many research groups.

This chapter deals with two of the aforementioned cases: the complete synchronization and the antisynchronization. In the case of complete synchronization, two identically coupled chaotic systems have a perfect coincidence of their chaotic trajectories, i.e., $x_1(t) = x_2(t)$ as $t \to \infty$. In the case of antisynchronization, for initial conditions chosen from large regions in the phase space two coupled systems x_1 and x_2, can be synchronized in amplitude, but with opposite sign, that is $x_1(t) = -x_2(t)$ as $t \to \infty$.

From our knowledge, chaotic systems exhibit high sensitivity on initial conditions or system's parameters and if they are identical and start from almost the same initial conditions, they follow trajectories which rapidly become uncorrelated. That is why many techniques exist to obtain chaotic synchronization. So, many of these techniques for coupling two or more nonlinear chaotic systems can be mainly divided into two classes: unidirectional coupling and bidirectional or mutual coupling [40]. In the first case, only the first system, the master system, drives the second one, the slave system, while in the second case, each system's dynamic behaviour influences the dynamics of the other.

Furthermore, the subject of synchronization between coupled chaotic systems, especially in the last decade, plays a crucial role in the field of neuronal dynamics [6, 41]. Neural signals in the brain are observed to be chaotic and it is worth considering further their possible synchronization [42–46]. These signals are produced by nerve membranes exhibiting their own nonlinear dynamics, which generate and propagate action potentials. Such nonlinear dynamics in nerve membranes can produce chaos in neurons and related bifurcations.

So, motivated by the aforementioned fact, the Birkhoff-Shaw system [45], which exhibits the structure of beaks and wings, typically observed in chaotic neuronal models, is chosen for use in this chapter. It is a second order non-autonomous dynamical system with rich dynamical

http://dx.doi.org/10.5772/64811

behaviour, which has not been sufficiently studied. Furthermore, the unidirectional coupling scheme, which is used, is designed by using the nonlinear controllers to target synchronization states, such as complete synchronization and antisynchronization, with amplification or attenuation in chaotic oscillators. The stability of synchronization is ensured by using Lyapunov function stability theorem in the unidirectional mode of coupling. The simulation results from system's numerical integration confirm the appearance of complete synchronization and antisynchronization phenomena depending on the signs of the parameters of the error functions. Electronic circuitry that models the coupling scheme is also reported to verify its feasibility.

This chapter is organized as follows. In Section 2, the features of chaotic systems and especially of the proposed Birkhoff-Shaw system by using various tools of nonlinear theory, such as bifurcation diagrams, phase portraits and Lyapunov exponents, are explored. The synchronization scheme, by using the nonlinear controller, as well as the unidirectional coupling scheme is discussed in Sections 3 and 4, respectively. The simulation results of the proposed method are presented for various cases in Section 5. Section 6 presents the circuital implementation of the coupling scheme and the results which are obtained by using the SPICE. Finally, the conclusive remarks and some thoughts for future works are drawn in the last section.

2. The Birkhoff-Shaw chaotic system

As it is known, chaos theory studies systems that present three very important features [46, 47]:

- its periodic orbits must be dense,
- it must be topologically mixing and
- it must be very sensitive on initial conditions.

In more details, the periodic orbits of a chaotic system have to be dense and that means that the trajectory of a dynamical system is dense, if it comes arbitrarily close to any point in the domain. The second feature of chaotic systems, the topological mixing, means that the chaotic trajectory at the phase space will move over time so that each designated area of this trajectory will eventually cover part of any particular region. Additionally, the third feature, which is the most important feature of chaotic systems, is the sensitivity on initial conditions. When a small variation on a system's initial conditions exists, a totally different chaotic trajectory will be produced.

Here, as it is mentioned above, the well-known non-autonomous chaotic system of Birkhoff-Shaw, which has been proposed by Shaw in 1981 [45], is used. The Birkhoff-Shaw system is described by the 2-D system of differential equations:

$$\begin{cases} \dot{x} = ay + x - cxy^2 \\ \dot{y} = -x - B\cos(dt) \end{cases} \tag{1}$$

where x and y are the states variables and a, B, c and d are positive parameters.

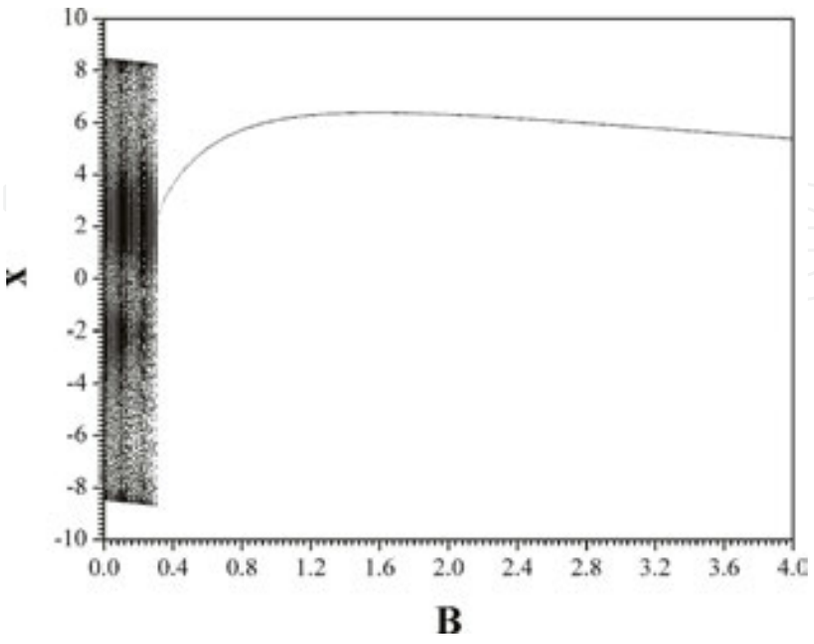

Figure 1. Bifurcation diagram of x versus B, for $a = 1$, $c = 0.1$ and $d = 1$.

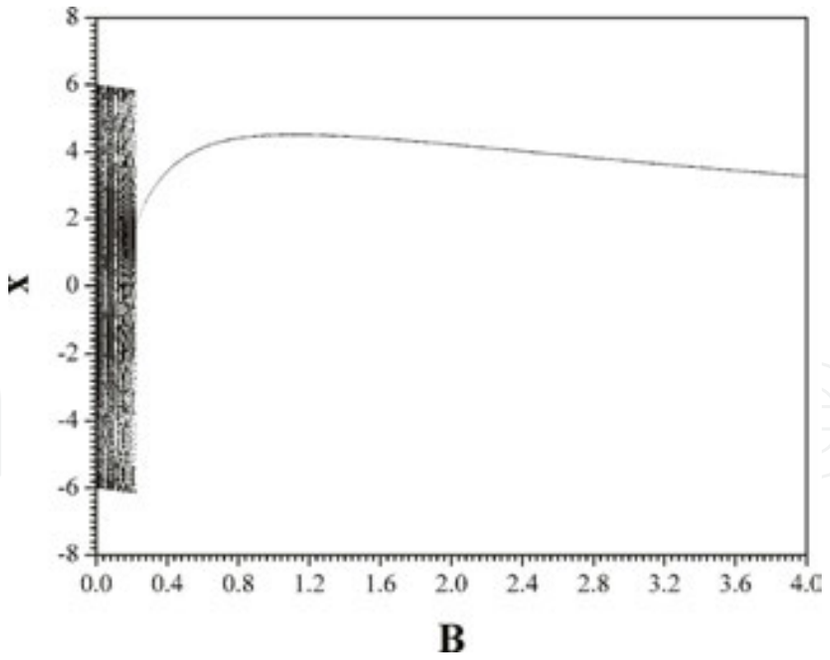

Figure 2. Bifurcation diagram of x versus B, for $a = 1$, $c = 0.2$ and $d = 1$.

In this section, the system's dynamic behaviour is investigated numerically by employing a fourth order Runge-Kutta algorithm. As a first step in this approach, the bifurcation diagram and the Lyapunov exponents, which are very useful tools from nonlinear theory, are used. In

http://dx.doi.org/10.5772/64811

Figures 1–8, two sets of bifurcation diagrams of the variable x versus the parameter B, for c = 0.1 and c = 0.2 and for various values of the parameter d, are displayed. The above bifurcation diagrams show the richness of system's dynamical behaviour. Apart from limit cycles, system (1) has quasiperiodicity and chaos, which makes the system's control a difficult target in practical applications where a particular dynamic is desired.

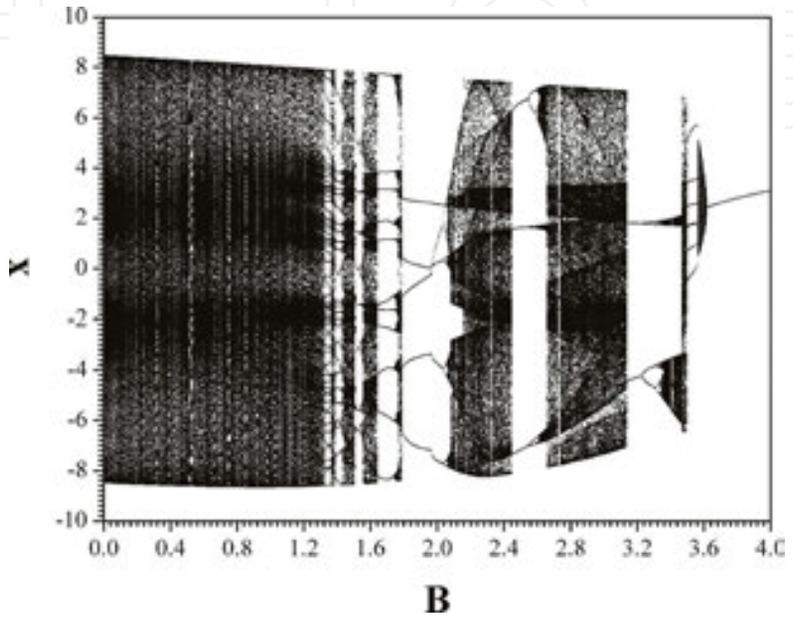

Figure 3. Bifurcation diagram of x versus B, for a = 1, c = 0.1 and d = 1.5.

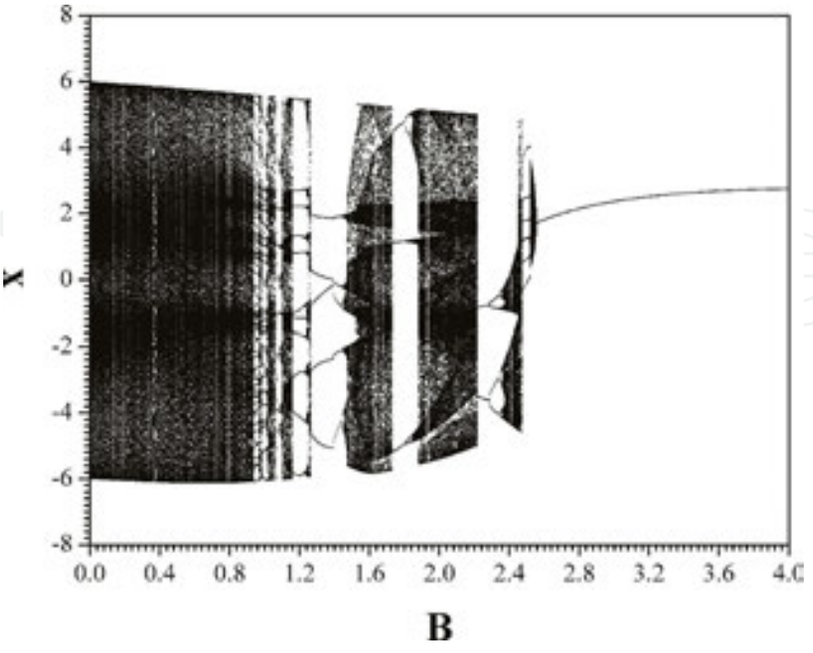

Figure 4. Bifurcation diagram of x versus B, for a = 1, c = 0.2 and d = 1.5.

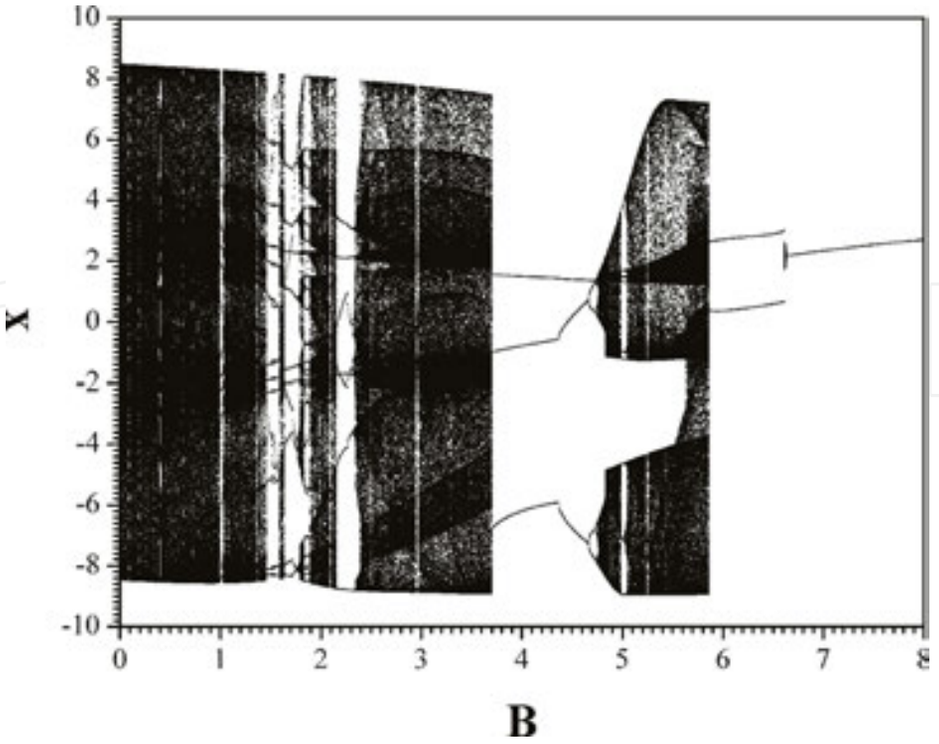

Figure 5. Bifurcation diagram of x versus B, for $a = 1$, $c = 0.1$ and $d = 2$.

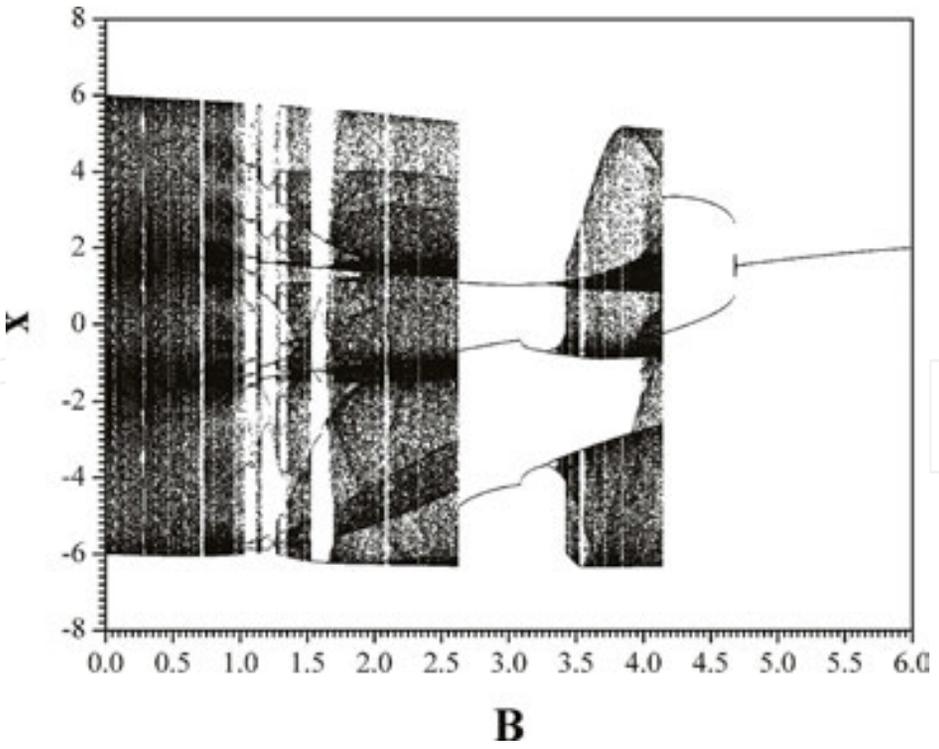

Figure 6. Bifurcation diagram of x versus B, for $a = 1$, $c = 0.2$ and $d = 2$.

http://dx.doi.org/10.5772/64811

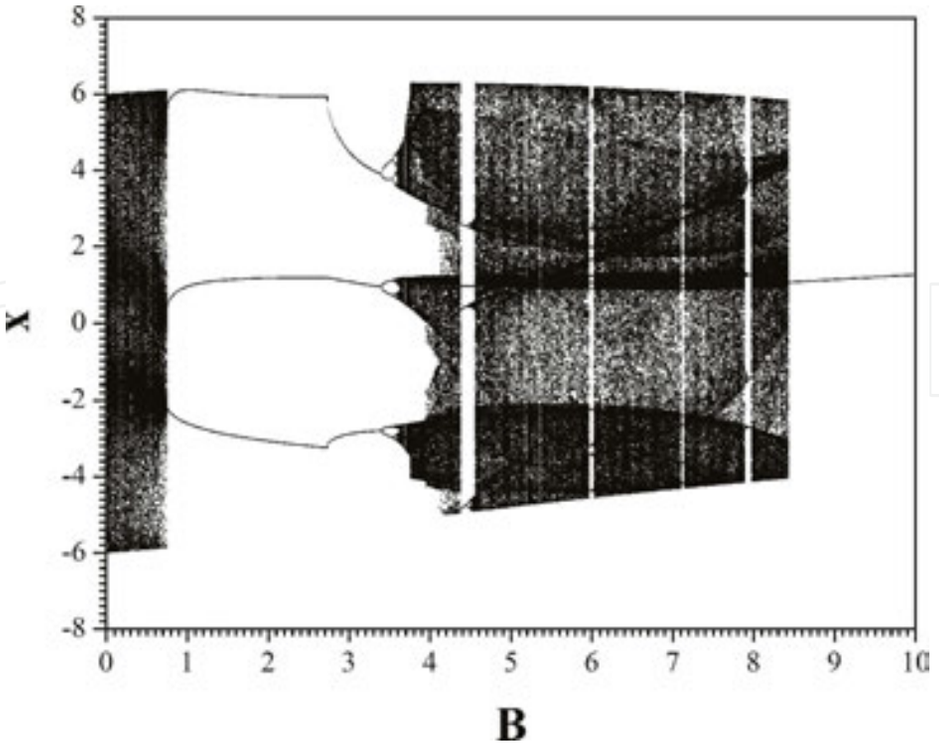

Figure 7. Bifurcation diagram of x versus B, for $a = 1$, $c = 0.1$ and $d = 3$.

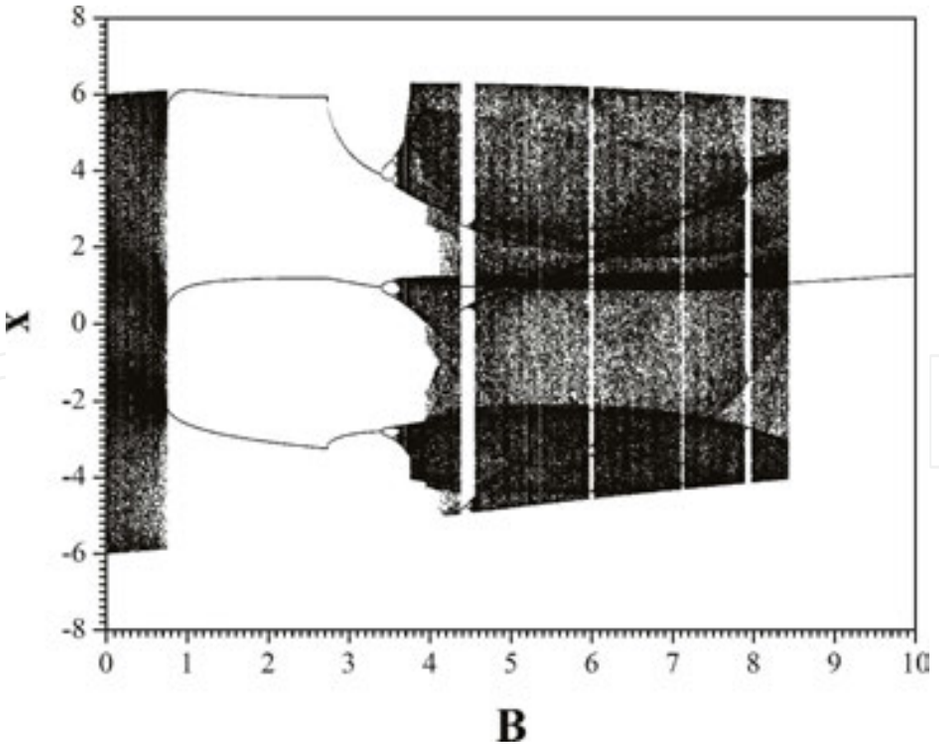

Figure 8. Bifurcation diagram of x versus B, for $a = 1$, $c = 0.2$ and $d = 3$.

In greater detail, having small values of the parameter d (i.e. $d = 1$) the system begins from a quasiperiodic state and as the amplitude B of the external force increases, the system passes to a stable periodic behaviour of period-1 (**Figures 1** and **2**). For example, in the case of $a = 1$, $c = 0.1$ and $d = 1$, the Lyapunov exponents (LEs) for two respective values of B in the regions of quasiperiodic and periodic regions are:

- for $B = 0.1$ (quasiperiodic state): $LE_1 = 0.000$, $LE_2 = 0.000$, $LE_3 = -1.516$
- for $B = 2$ (periodic state): $LE_1 = 0.000$, $LE_2 = -0.996$, $LE_3 = -80.998$

According to the nonlinear theory, if the number of zeros of LEs is one or two then the system is in periodic or quasiperiodic behaviour, respectively. So, the calculation of Lyapunov exponents plays a crucial role to the estimation of the dynamic behaviour of the proposed system.

However, as the value of the parameter d increases the system's complexity is also increased. For $d = 1.5$ (**Figures 3** and **4**) in both cases of $c = 0.1$ and $c = 0.2$, the range of quasiperiodic region has been significantly enlarged, as compared to the previous case ($d = 1$). Nevertheless, with the end of this region, system's behaviour alternates between periodic and chaotic ones. The chaotic regions are detected by finding one positive Lypaunov exponent (i.e. for $a = 1$, $B = 2.8$, $c = 0.1$ and $d = 1.5$, the Lypaunov exponents are: $LE_1 = 0.157$, $LE_2 = 0.000$, $LE_3 = -1.626$). Finally, the system passes from a quasiperiodic state to a stable periodic (period-1) one again.

System's behaviour remains almost the same as the value of parameter d (i.e. $d = 2$) increases (**Figures 5** and **6**). However, two important conclusions could be drawn. The first is that the chaotic regions have been enlarged, while the second is that the quasiperiodic region, before the final system's periodic state, has been significantly decreased.

Finally, if the value of parameter d has been further increased(i.e. $d = 3$) then the chaotic regions have also been increased while the respective periodic regions have been significantly decreased. Also, the system suddenly passes from chaotic to the final periodic behaviour, as it is shown in the bifurcation diagram of **Figures 7** and **8**.

In these diagrams, the region of period-3 dominates, which is characteristic of system's chaotic behaviour. Also, this region reveals two more important phenomena from nonlinear theory. Firstly, this window of period-3 begins with a sudden transition from a chaotic to periodic behaviour, which in this case is known as *Intermittency* [48] and ends with an *Interior Crisis* [49, 50] that causes intermittency induced from crisis.

In **Figures 9–12**, the phase portraits for various values of the parameter B, in the case of $a = 1$, $c = 0.2$ and $d = 3$, are presented. In more details, **Figure 9** shows the quasiperiodic attractor, that the system is in for low values of the amplitude B ($B = 0.5$) of the external sinusoidal source, while **Figures 10** and **12** display the system's periodic attractors of period-3 ($B = 3$) and period-1 ($B = 9$), respectively. Finally, in **Figure 11** the system's chaotic attractor for $B = 7$ is presented.

http://dx.doi.org/10.5772/64811

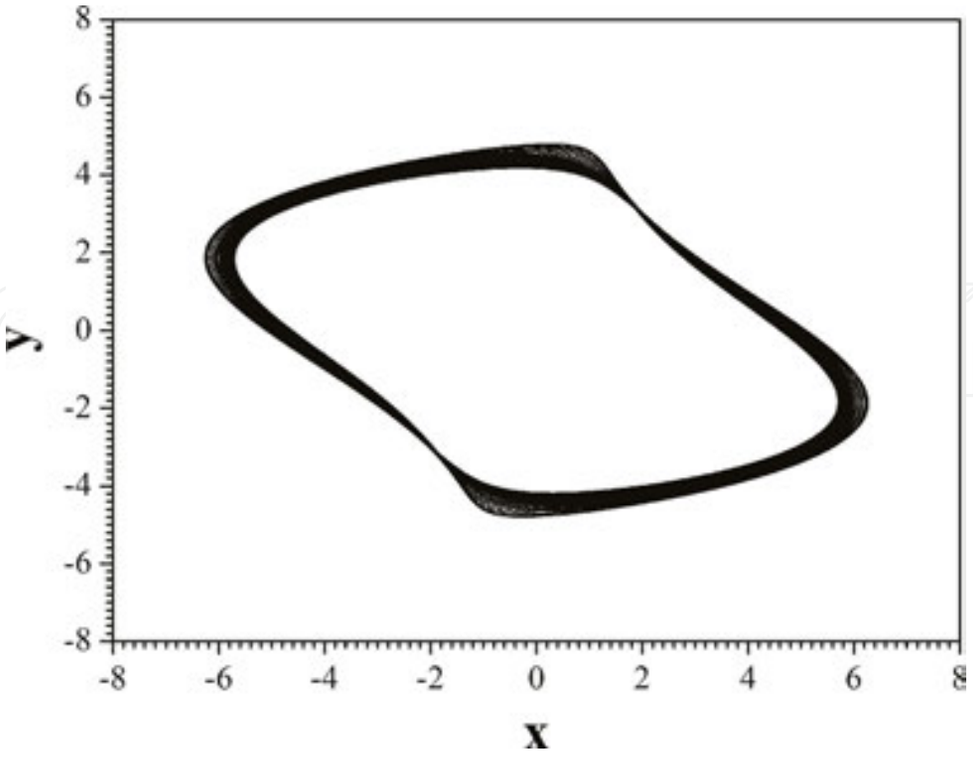

Figure 9. Phase portrait of y versus x, for $a = 1$, $c = 0.2$, $d = 3$ and $B = 0.5$ (quasiperiodic behaviour).

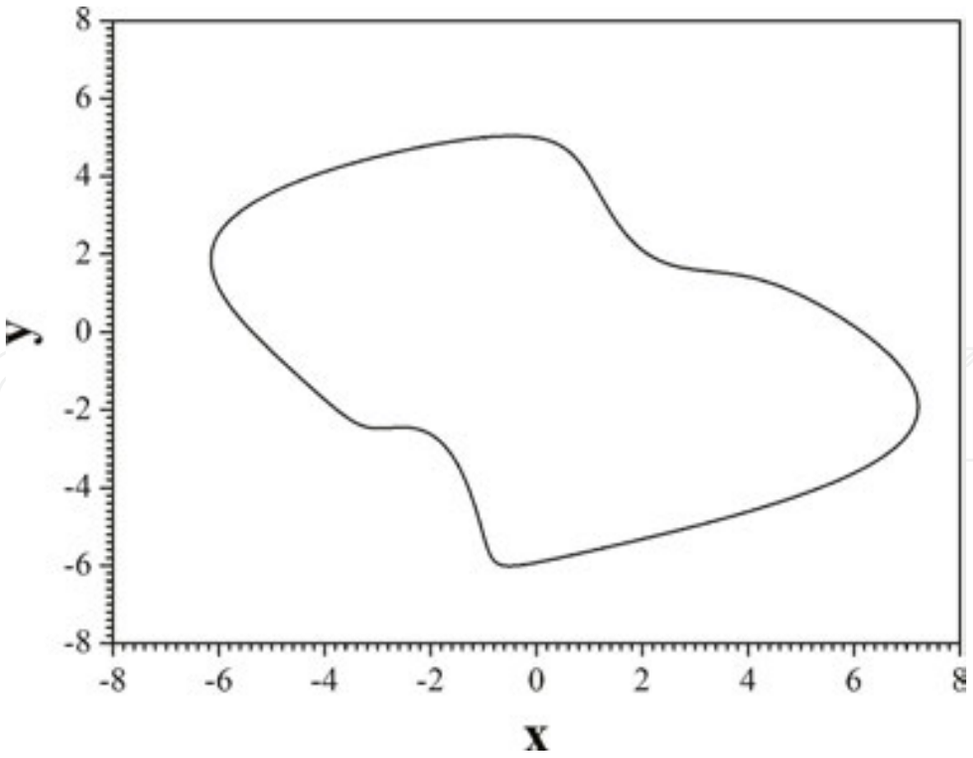

Figure 10. Phase portrait of y versus x, for $a = 1$, $c = 0.2$, $d = 3$ and $B = 3$ (periodic behaviour).

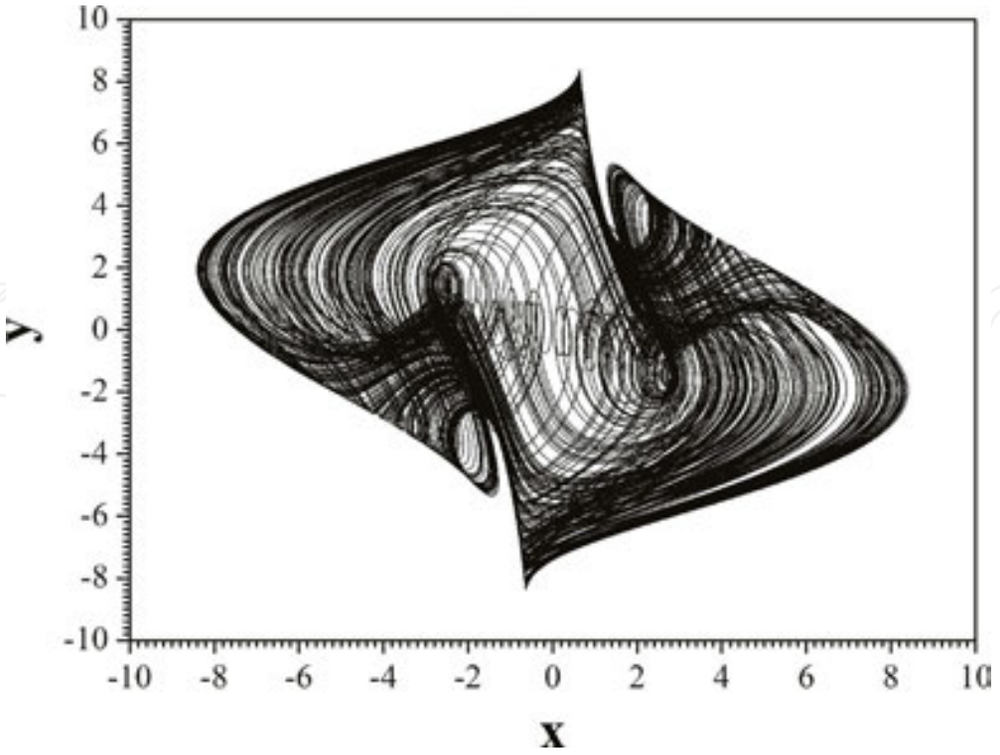

Figure 11. Phase portrait of y versus x, for $a = 1$, $c = 0.2$, $d = 3$ and $B = 7$ (chaotic behaviour).

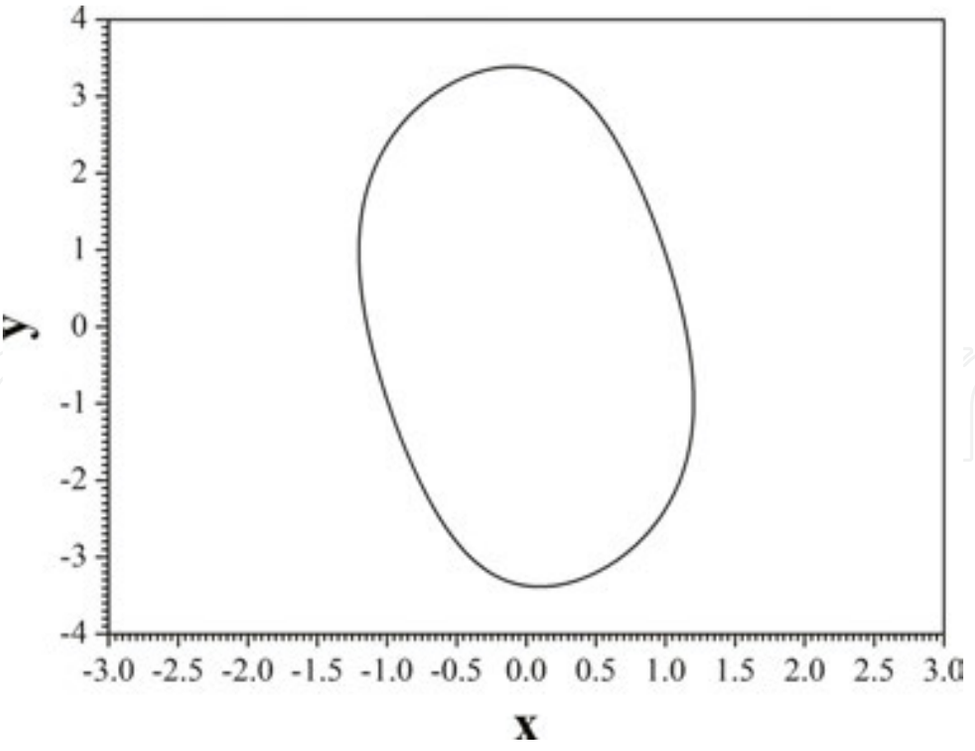

Figure 12. Phase portrait of y versus x, for $a = 1$, $c = 0.2$, $d = 3$ and $B = 9$ (periodic behaviour).

http://dx.doi.org/10.5772/64811

3. The proposed coupling scheme

Two identical unidirectionally coupled chaotic systems can be described by the following system of differential equations:

$$\begin{cases} \dot{x} = f(x) + U_X \\ \dot{y} = f(y) + U_Y \end{cases} \tag{2}$$

where $(f(x), f(y)) \in R^n$ are the flows of the systems. Nonlinear controllers (NCs), U_X and U_Y, define the coupling of the systems, while the error function is given by $e = ky - lx$, where k and l are constants [51, 52]. If the Lyapunov function stability (LFS) technique is applied, a stable synchronization state will be obtained when the error function of the coupled system follows the limit:

$$\lim_{t\to\infty} \|e(t)\| \to 0 \tag{3}$$

so that $lx = ky$.

The design process of the coupling scheme, is based on the Lyapunov function:

$$V(e) = \frac{1}{2} e^T e \tag{4}$$

where T is a transpose of a matrix and $V(e)$. The Lyapunov function (4) is a positive definite function. Also, for known system's parameters and with the appropriate choice of the controllers U_X and U_Y, the coupled system has $V(e) < 0$. This ensures the asymptotic global stability of synchronization and thereby realizes any desired synchronization state [51, 52].

By using the appropriate NCs functions U_X, U_Y and error function's parameters k, l, a bidirectional (mutual) or unidirectional coupling scheme can be implemented. Analytically, while if $U_{X,Y} \neq 0$ and $k, l \neq 0$, a bidirectional coupling scheme is realized, while if ($U_X = 0$, $k = 1$) or ($U_Y = 0$, $l = 1$), a unidirectional coupling scheme is realized, respectively. The signs of the constants k, l play a crucial role to the synchronization case (complete synchronization or antisynchronization), which is observed in this work. However, the ratio of k over l decides the amplification of one oscillator relative to another one.

Next, the simulation results in the unidirectional coupling scheme and for various values of parameters k and l are presented in details.

4. Unidirectional coupling

In this section, the unidirectional coupling scheme for $U_X = 0$, in the case of coupled systems of Eq. (1), is presented. The coupled system is described by the following systems of Eqs. (5) and (6).

Master system:

$$\begin{cases} \dot{x}_1 = ax_2 + x_1 - cx_1x_2^2 \\ \dot{x}_2 = -x_1 - B\,cos(dt) \end{cases} \tag{5}$$

Slave system:

$$\begin{cases} \dot{y}_1 = ay_2 + y_1 - cy_1y_2^2 + U_{Y1} \\ \dot{y}_2 = -y_1 - B\,cos(dt) + U_{Y2} \end{cases} \tag{6}$$

where $\boldsymbol{U}_Y = [U_{Y1}, U_{Y2}]^T$ is the Nonlinear Controller (NC). The error function is defined by $\boldsymbol{e} = k\boldsymbol{y} - l\boldsymbol{x}$, with $\boldsymbol{e} = [e_1, e_2]^T$, $\boldsymbol{x} = [x_1, x_2]^T$ and $\boldsymbol{y} = [y_1, y_2]^T$. So, the error dynamics, by taking the difference of Eqs. (5) and (6), are written as:

$$\begin{cases} \dot{e}_1 = ae_2 + e_1 + lcx_1x_2^2 - kcy_1y_2^2 + kU_{Y1} \\ \dot{e}_2 = -e_1 - B(k-l)\cos(dt) + kU_{Y2} \end{cases} \tag{7}$$

For stable synchronization, $e \to 0$ as $t \to \infty$. By substituting the conditions in Eq. (7) and taking the time derivative of Lyapunov function

$$\begin{aligned} &\dot{V}(e) = e_1\dot{e}_1 + e_2\dot{e}_2 = \\ &= e_1\left(ae_2 + e_1 + lcx_1x_2^2 - kcy_1y_2^2 + kU_{Y1}\right) + e_2\left(-e_1 - B(k-l)\,cos(dt) + kU_{Y2}\right) \end{aligned} \tag{8}$$

We consider the following NC controllers:

$$\begin{cases} U_{Y1} = -\dfrac{1}{k}(ae_2 + 2e_1 + lcx_1x_2^2 - kcy_1y_2^2) \\ U_{Y2} = -\dfrac{1}{k}\left(-e_1 - B(k-l)\cos(dt) + e_2\right) \end{cases} \tag{9}$$

such that

http://dx.doi.org/10.5772/64811

$$\dot{V}(e) = -e_1^2 - e_2^2 < 0 \tag{10}$$

Eq. (10) ensures the asymptotic global stability of synchronization.

5. Simulation results

In this section, the simulation results, with the unidirectional coupling scheme, in three different cases are presented.

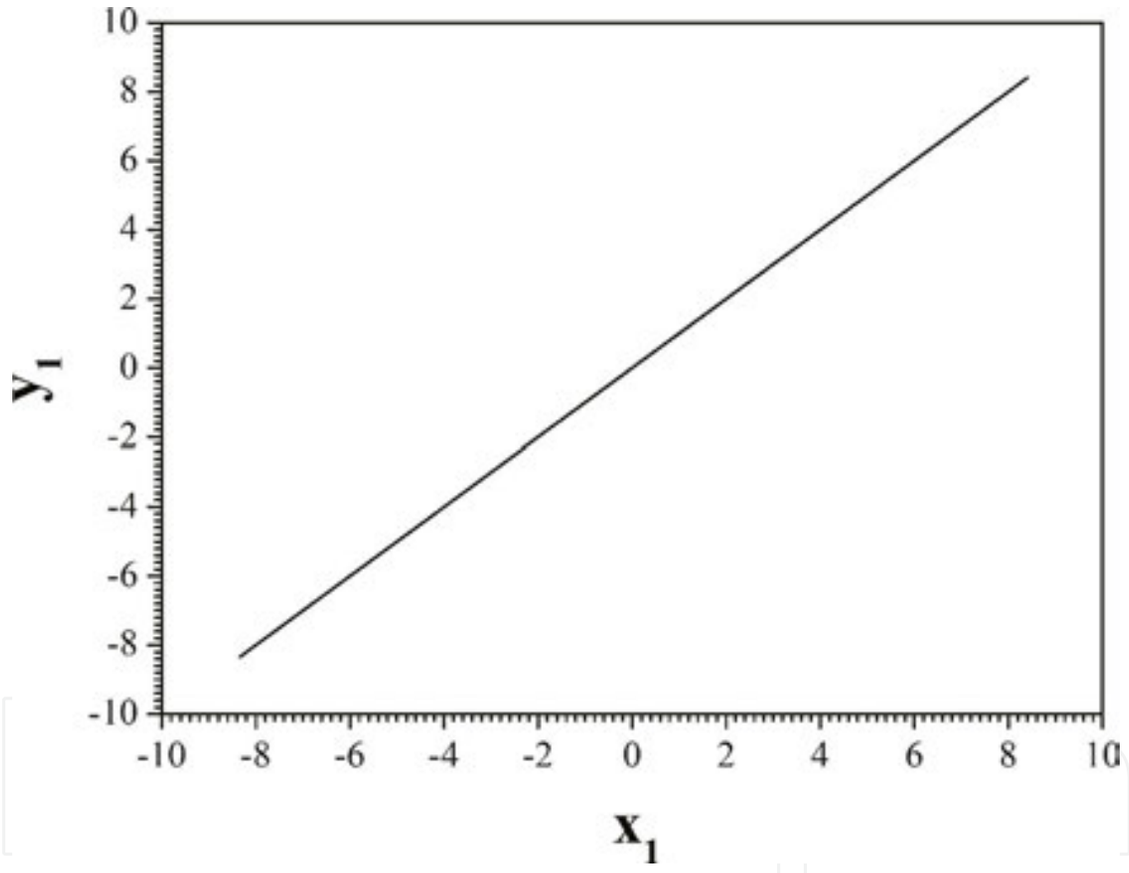

Figure 13. The phase portrait of y_1 versus x_1, for $a = 1$, $B = 7$, $c = 0.2$ and $d = 3$.

5.1. The case for $k = l = 1$

As it is mentioned, the phenomenon of complete synchronization is achieved for every value of k, l. Especially for $k = -l = 1$, the two coupled systems are in the chaotic state, due to the chosen values of system's parameters ($a = 1$, $B = 7$, $c = 0.2$ and $d = 3$) and initial conditions (x_1, x_2, y_1, y_2) = (3, 2, –1, –5). The goal of complete synchronization is achieved as it is shown from the plots of y_1 versus x_1, the time-series of x_2, y_2 and the errors e_i in **Figures 13–15**.

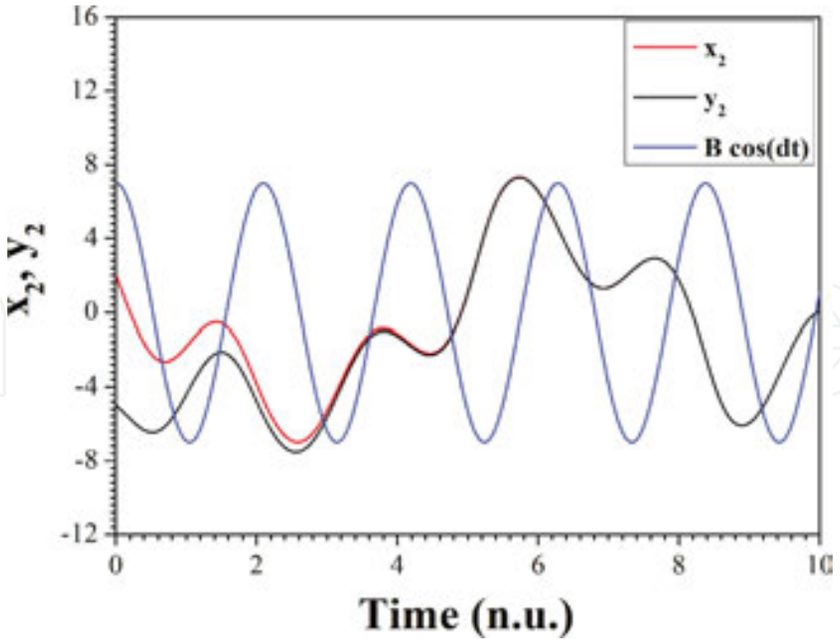

Figure 14. The time-series of x_2, y_2, in regards to the external periodic signal, for $a = 1$, $B = 7$, $c = 0.2$ and $d = 3$.

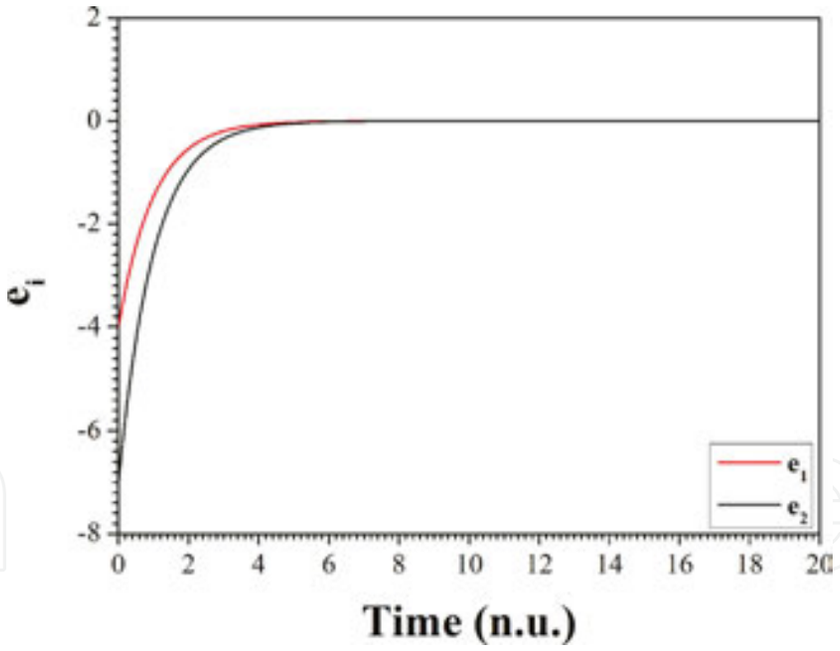

Figure 15. The time-series of errors e_1, e_2, with $k = l = 1$, for $a = 1$, $B = 7$, $c = 0.2$ and $d = 3$.

5.2. The case for $k = l = 1$

In the second case, by using opposing values for the parameters $k = -l = 1$ and for the same values of system's parameters ($a = 1$, $B = 7$, $c = 0.2$ and $d = 3$), the phenomenon of antisynchronization is achieved. This conclusion is derived from the phase portrait of y_1 versus x_1

http://dx.doi.org/10.5772/64811

(**Figure 16**), as well as from the time series of x_2, y_2 (**Figure 17**). Also, the plot of errors $e_i = y_i + x_i$ in **Figure 18** confirms the antisynchronization of the coupled system.

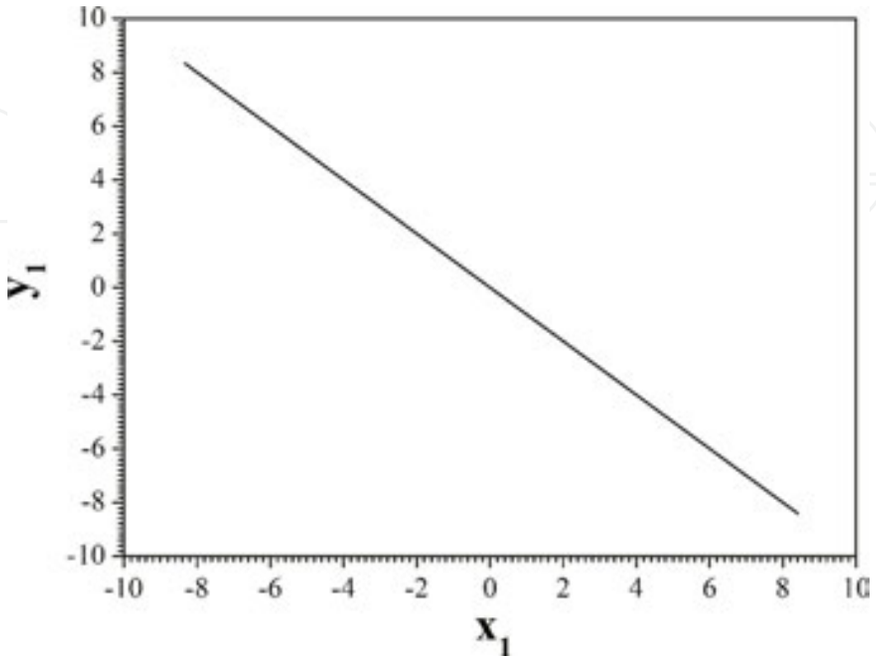

Figure 16. The phase portrait of y_1 versus x_1, for $a = 1$, $B = 7$, $c = 0.2$ and $d = 3$.

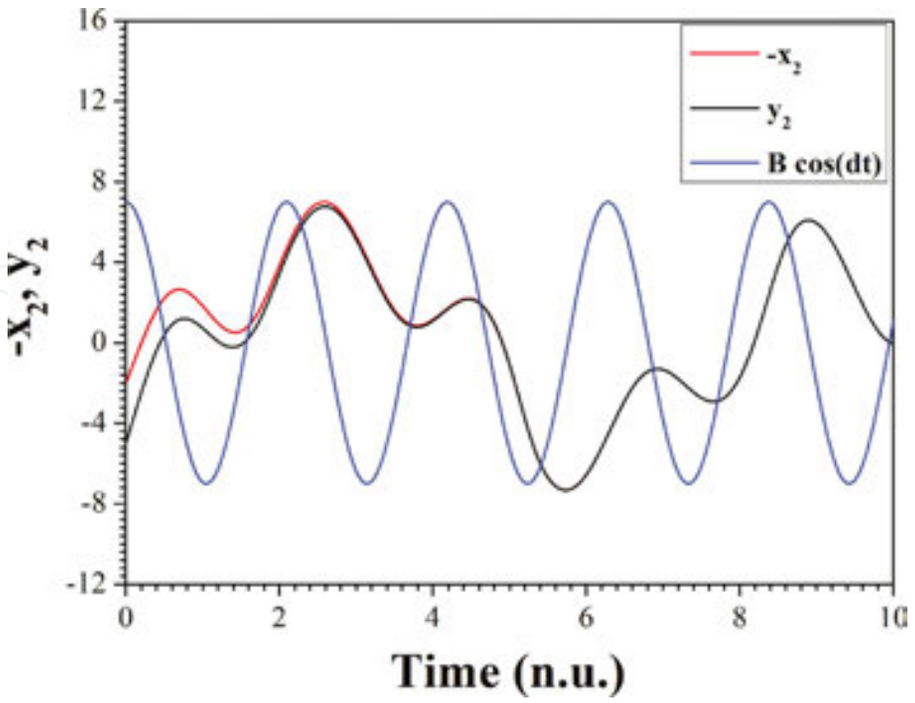

Figure 17. The time-series of $-x_2$, y_2, in regard to the external periodic signal, for $a = 1$, $B = 7$, $c = 0.2$ and $d = 3$.

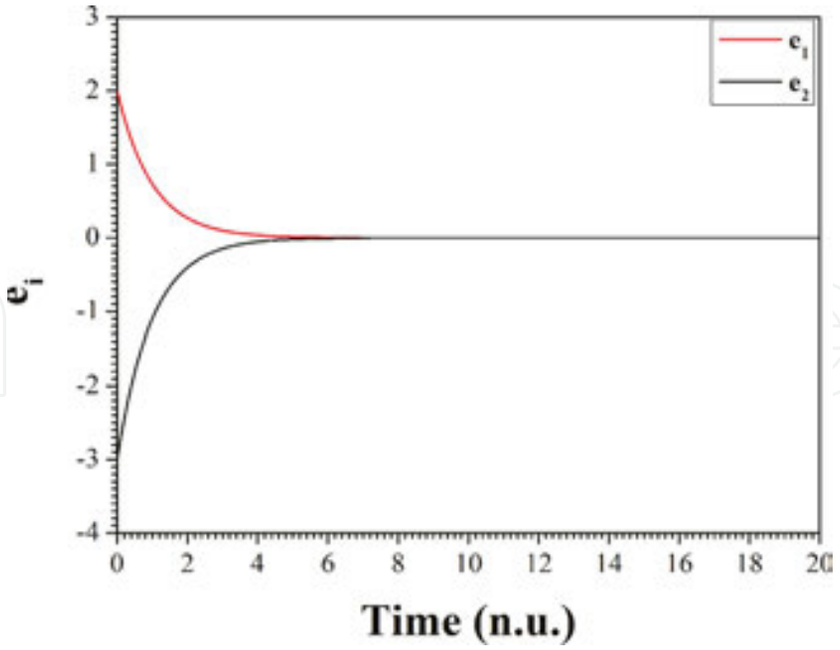

Figure 18. The time-series of errors e_1, e_2, with $k = l = 1$, for $a = 1$, $B = 7$, $c = 0.2$ and $d = 3$.

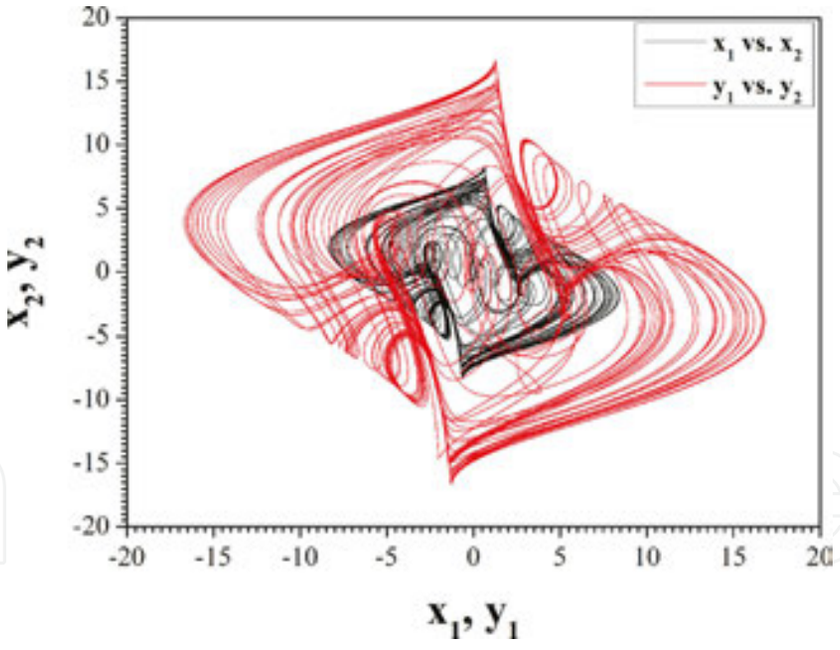

Figure 19. The phase portraits of x_2 versus x_1(black colour) and y_2 versus y_1 (red colour), for $a = 1$, $B = 7$, $c = 0.2$ and $d = 3$.

5.3. The case for $k = 1$, $l = 2$

In this case, the parameters of the error functions are chosen as $k = 1$ and $l = 2$. By choosing the systems' parameters as $a = 1$, $B = 7$, $c = 0.2$ and $d = 3$ the chaotic attractor of the second system is enlarged by two times, as it is shown with red colour in **Figure 19**, as well as by the time-

http://dx.doi.org/10.5772/64811

series of signals x_2 and y_2 (**Figure 21**). The y_1 versus x_1 plot in **Figure 20** confirms that the coupled system is in complete synchronization state independently of the values of the error's parameters k, l. The error plot $e_i = y_i - 2x_i$ ($i = 1, 2$) in **Figure 22** shows the exponential convergence to zero that confirms the realization of system's complete synchronization state.

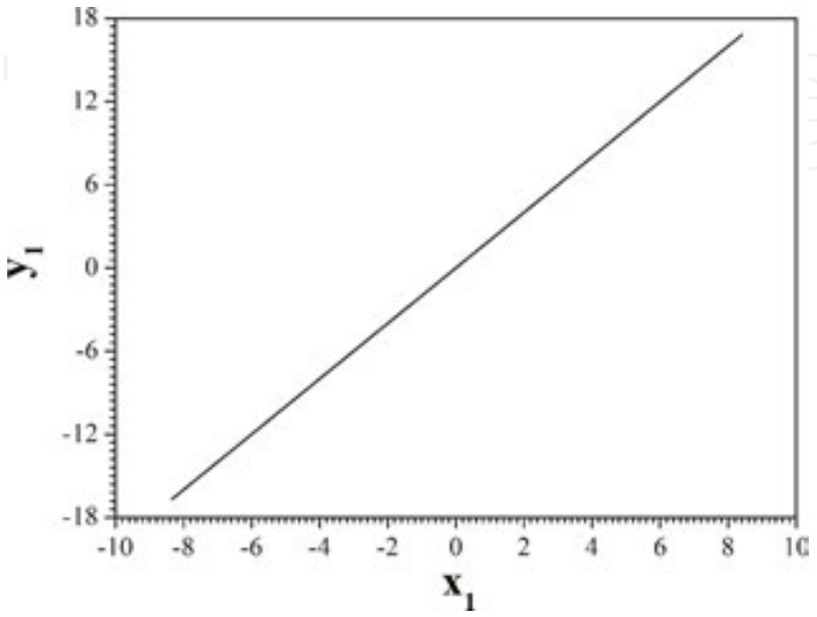

Figure 20. The phase portrait of y_1 versus x_1, for $a = 1$, $B = 7$, $c = 0.2$ and $d = 3$.

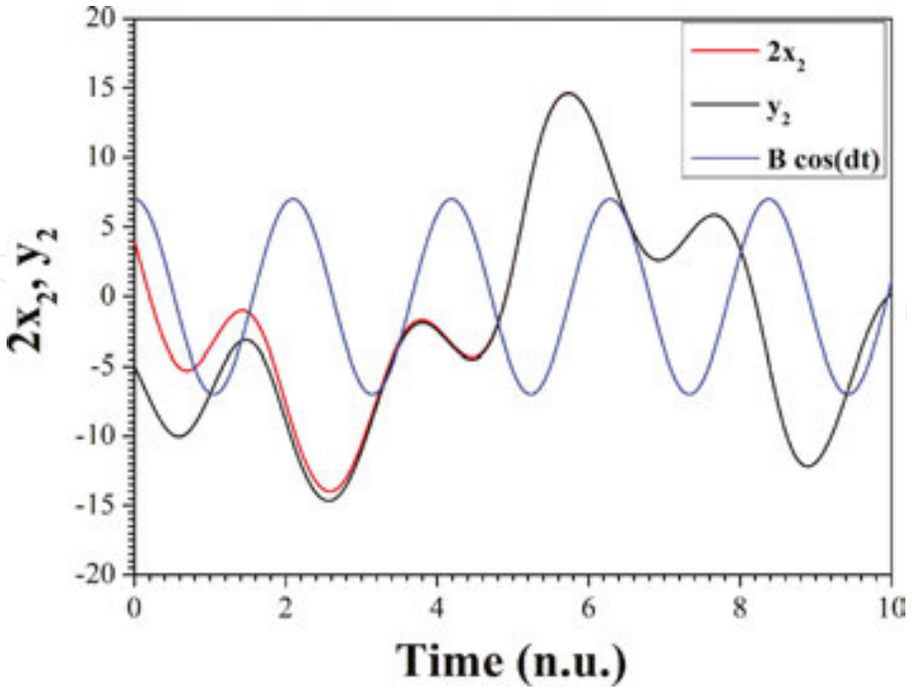

Figure 21. The time-series of $2x_2$, y_2, in regard to the external periodic signal, for $a = 1$, $B = 7$, $c = 0.2$ and $d = 3$.

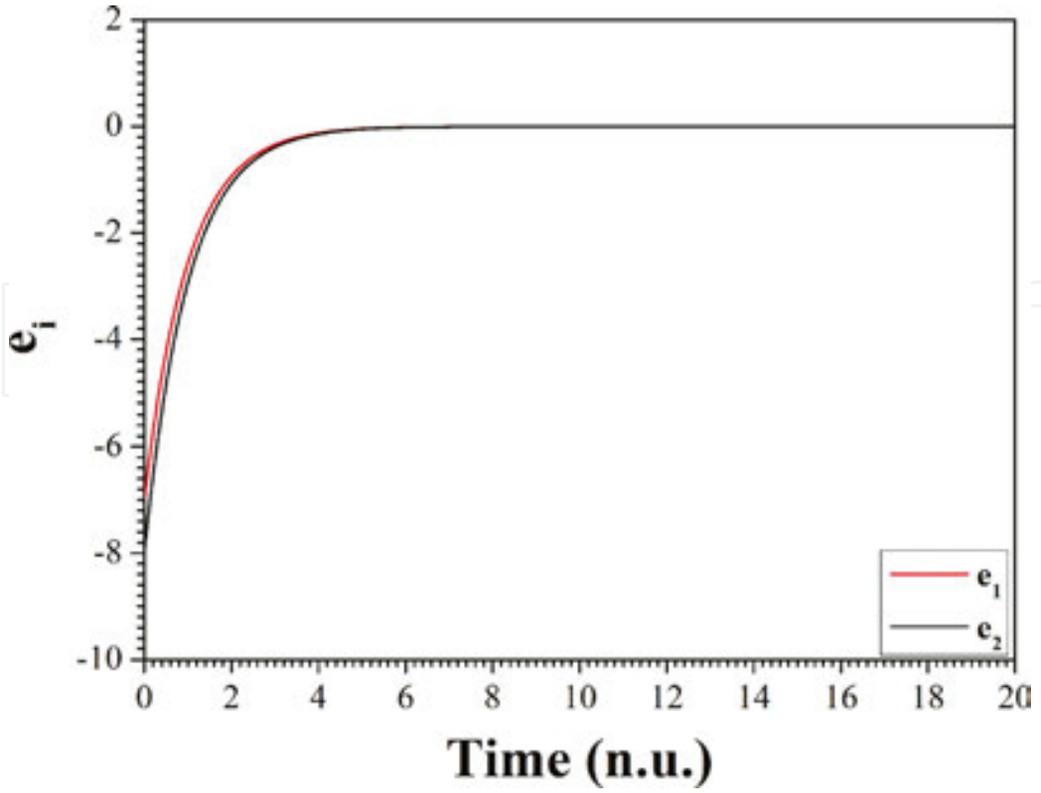

Figure 22. The time-series of errors e_1, e_2, with $k = 1$, $l = 2$, for $a = 1$, $B = 7$, $c = 0.2$ and $d = 3$.

6. Circuit's implementation of the coupling scheme

The circuit implementation of the proposed synchronization coupling scheme, with the electronic simulation package Cadense OrCAD, for $k = l = 1$, is presented in this section, in order to prove the feasibility of the proposed method. The coupling system's circuitry design consists of three sub-circuits, which are the master circuit, the coupling circuit and the slave circuit. Also, the circuit is realized by using common electronic components.

Figure 23 shows the schematic of the master circuit, which has two integrators (U_1 and U_2) and one differential amplifier (U_3), which are implemented with the TL084, as well as two signals multipliers (U_4, U_5) by using the AD633. By applying Kirchhoff's circuit laws, the corresponding circuital equations of designed master circuit can be written as:

$$\begin{cases} \dot{x}_1 = \dfrac{1}{RC}\left(x_2 + x_1 - \dfrac{R}{100R_1} x_1 x_2^2 \right) \\ \dot{x}_2 = \dfrac{1}{RC}\left(-x_1 - V_0 \cos(\omega t) \right) \end{cases} \tag{11}$$

http://dx.doi.org/10.5772/64811

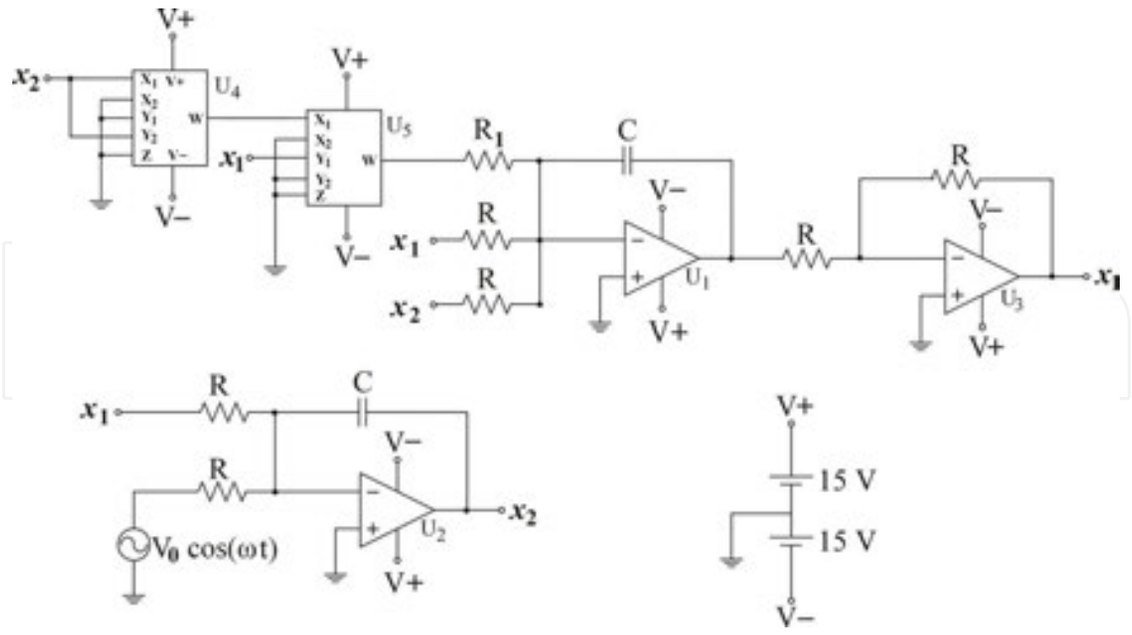

Figure 23. The schematic representation of the master circuit.

where x_i (i = 1, 2) are the voltages in the outputs of the operational amplifiers U_3 and U_2. Normalizing the differential equations of system (18) by using $\tau = T/RC$ we could see that this system is equivalent to the system (12). The circuit components have been selected as: R = 10 kΩ, R_1 = 500 Ω, C = 10 nF, V_0 = 7 V and f = 4777 Hz, while the power supplies of all active devices are ±17 V_{DC}. For the chosen set of components the master system's parameters are: a = 1, B = 7, c = 0.2 and d = 3. In **Figure 24**, the chaotic attractor, which is obtained from Cadence OrCAD in (x_1, x_2) phase plane, is proved to be in a very good agreement with the respective phase portrait from system's numerical simulation process (**Figure 11**). So, the proposed circuit emulates very well the master system.

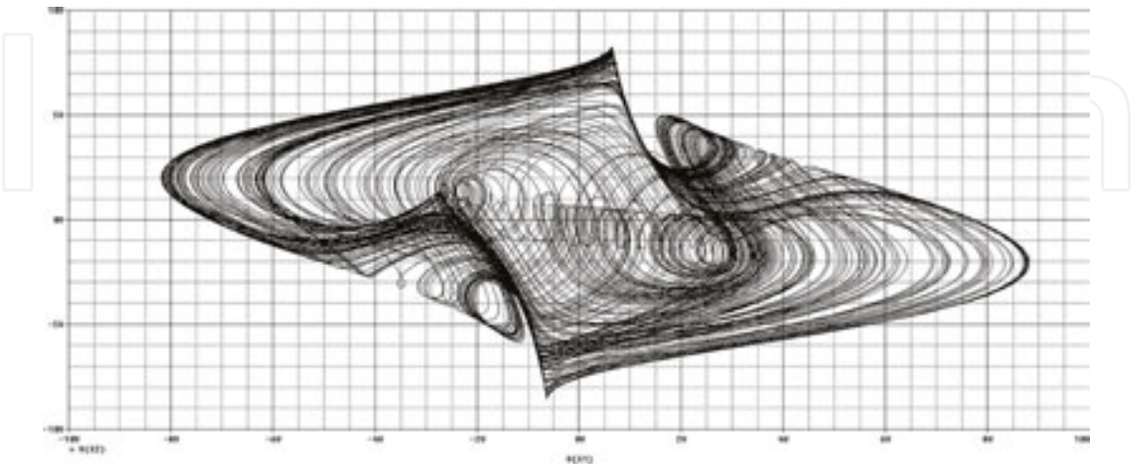

Figure 24. The chaotic attractor produced by the designed master circuit, obtained from Cadence OrCAD in the (x_1, x_2) phase plane.

In **Figure 25**, the schematic of the slave circuit, which is similar to the master circuit, is shown. The difference of this circuit in comparison to the previous one are the signals u_1 and mu_2, where u_1 is the control signal U_{Y1} and mu_2 is the opposite, due to the integrator, of the signal U_{Y2}, of system (6). So, for $k = l = 1$, the signal mu_2 is given as

$$mu_2 = -e_1 + e_2 \tag{12}$$

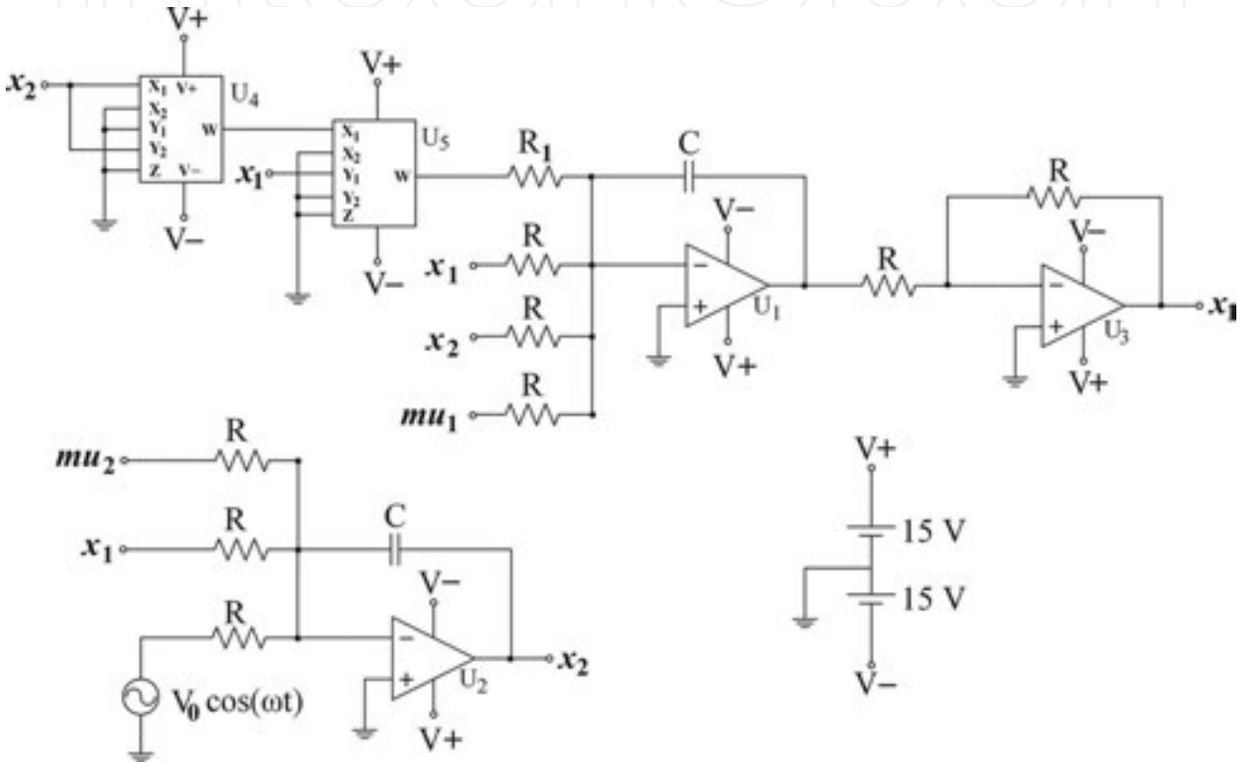

Figure 25. The schematic representation of the slave circuit.

The dynamics of the slave circuit is described by the following set of differential equations.

$$\begin{cases} \dot{y}_1 = \dfrac{1}{RC}\left(y_2 + y_1 - \dfrac{R}{100R_1} y_1 y_2^2 + u_1 \right) \\ \dot{y}_2 = \dfrac{1}{RC}\left(-y_1 - V_0 \cos(\omega t) - mu_2 \right) \end{cases} \tag{13}$$

Finally, the units from which the coupling circuit is consisted, are shown in the schematic of **Figure 26**, in which e_i, ($i = 1, 2$) are the difference signals ($e_i = ky_i - lx_i$, $i = 1, 2$), with $k = l = 1$ and me_2 is the opposite of e_2. Also, the resistors $R_2 = 5\,\text{k}\Omega$ and $R_3 = 50\,\text{k}\Omega$ have been used for achieving the desired values of system's parameters.

http://dx.doi.org/10.5772/64811

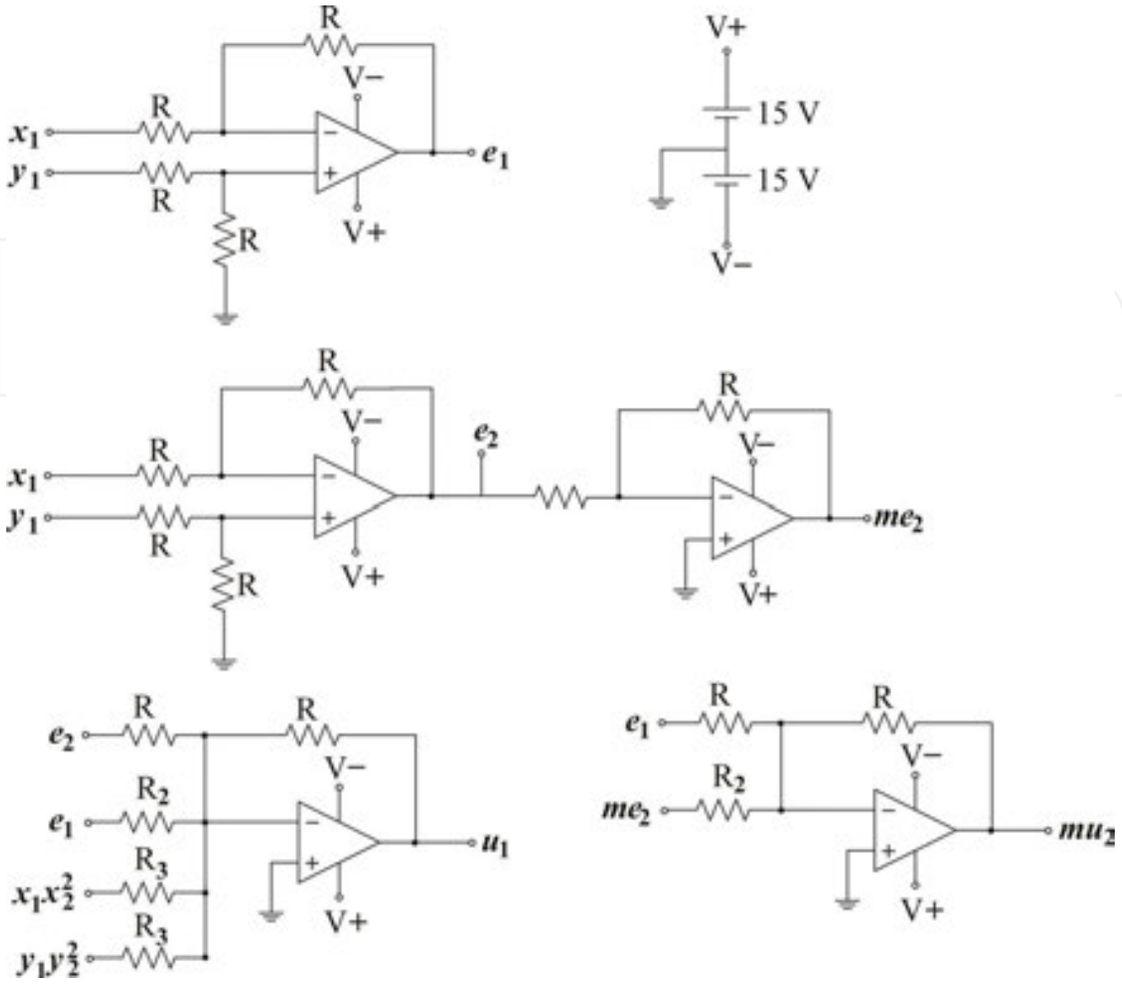

Figure 26. The schematic representation of the coupling circuit.

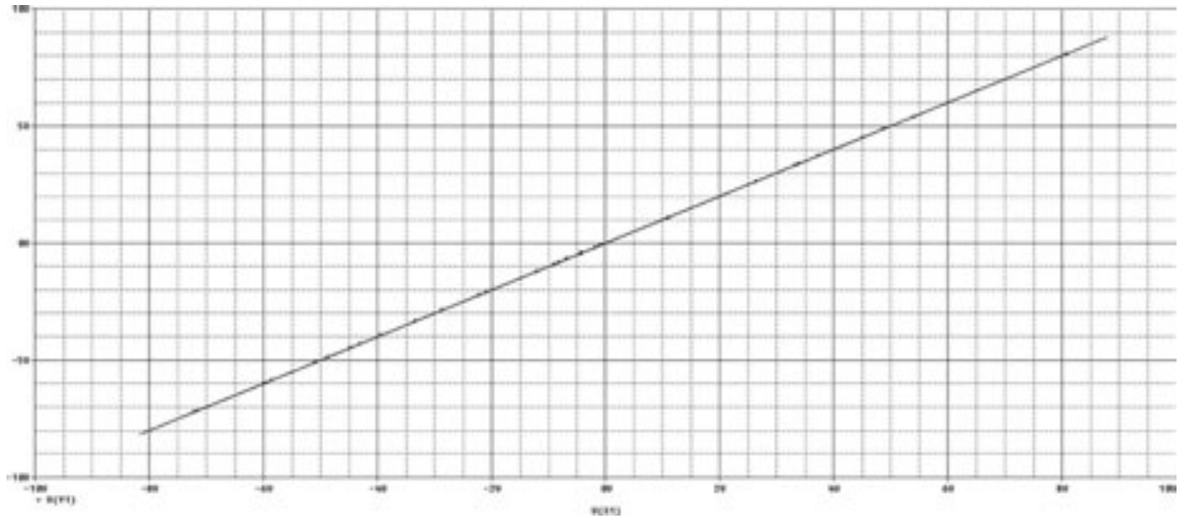

Figure 27. The phase portrait of y_1 vs. x_1, for $a = 1$, $B = 7$, $c = 0.2$ and $d = 3$, obtained from Cadence OrCAD.

Figures 27 and **28** depict the phase portraits in (x_i, y_i) phase planes, with i = 1, 2, for a = 1, B = 7, c = 0.2 and d = 3, obtained from Cadence OrCAD. These figures confirm the achievement of complete synchronization in the case of unidirectionally coupled circuits with the proposed method.

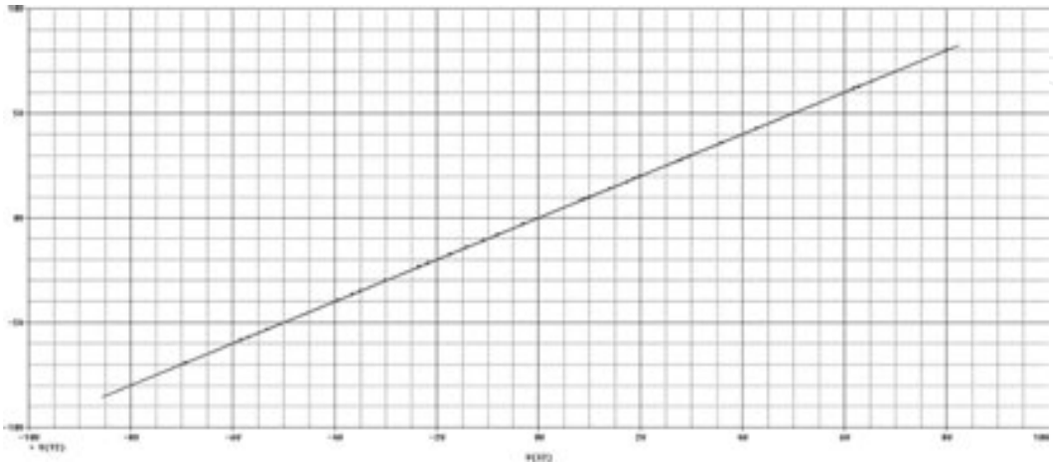

Figure 28. The phase portrait of y_2 versus x_2, for a = 1, B = 7, c = 0.2 and d = 3, obtained from Cadence OrCAD.

7. Conclusion

In this chapter, the case of unidirectional coupling scheme of two chaotic non-autonomous dynamical systems was studied. The proposed system is the second order Birkhoff-Shaw system, which is simple but very interesting from the perspective of nonlinear analysis. Furthermore, the coupling method was based on a recently new proposed scheme based on the nonlinear controller, which is applied for the first time in non-autonomous systems.

The Birkhoff-Shaw system is one of the simplest 2-D nonlinear systems exhibiting a rich dynamical behaviour. Besides limit cycles, Birkhoff-Shaw system presents quasiperiodicity and chaos, which can make the control of the system a difficult target in practical applications, where a particular dynamic is desired. Also, two well-known phenomena of nonlinear theory, the Intermittency and the Interior Crisis have been observed. However, the main drawback of this system is the fact that this system is a non-autonomous dynamical system, which makes the coupling method weak, especially if it is used in secure communication schemes.

In agreement to the simulation results, the circuital implementation of the proposed system in SPICE, in the case of unidirectional coupling, confirms the appearance of complete synchronization and antisynchronization, depending on the signs of the parameters of the error functions, in various cases. With this method, by choosing an appropriate sign for the error functions, the coupling system can be driven either to complete synchronization or antisynchronization behaviour.

http://dx.doi.org/10.5772/64811

From our knowledge, the complex behaviour of chaotic systems, like the ones that mentioned above, makes the synchronization difficult in practical applications where a particular dynamic is desired. For this reason, the synchronization of chaotic systems has attracted considerable attention due to its great potential applications, in secure communication, chemical reactions and biological systems. Especially, the synchronization in coupled neurons is a subject of a growing interest in the research community. So, due to the fact that Birkhoff-Shaw chaotic attractor exhibits the structure of beaks and wings, typically observed in chaotic neuronal models, the proposed coupling scheme showed an interesting research result of achieving the synchronization or antisynchronization in the case of coupled neuronal models.

As a next step in this direction is the application of the proposed method in non-identical Birkhoff-Shaw coupled systems in order to satisfy the goal of control of systems, which are in totally different dynamical behaviours. Also, the case of bidirectional coupling as well as the case of generalized synchronization, with the proposed scheme, could be examined.

Author details

Christos K. Volos[1], Hector E. Nistazakis[2*], Ioannis M. Kyprianidis[1], Ioannis N. Stouboulos[1] and George S. Tombras[2]

*Address all correspondence to: enistaz@phys.uoa.gr

1 Physics Department, Aristotle University of Thessaloniki, Thessaloniki, Greece

2 Department of Electronics, Computers, Telecommunications and Control, Faculty of Physics, National and Kapodistrian University of Athens, Athens, Greece

References

[1] Holstein-Rathlou NH, Yip KP, Sosnovtseva OV, Mosekilde E. Synchronization phenomena in nephron-nephron interaction. Chaos. 2001;11:417–426.

[2] Mosekilde E, Maistrenko Y, Postnov D, editors. Chaotic synchronization: applications to living systems. Singapore: World Scientific; 2002. 440 p.

[3] Pikovsky AS, Rosenblum M, Kurths J, editors. Synchronization: a universal concept in nonlinear sciences. Cambridge: Cambridge University Press; 2003. 433 p.

[4] Szatmári I, Chua LO. Awakening dynamics via passive coupling and synchronization mechanism in oscillatory cellular neural/nonlinear networks. Int. J. Circ. Theor. Appl. 2008;36:525–553.

[5] Tognoli E, Kelso JAS. Brain coordination dynamics: true and false faces of phase synchrony and metastability. Prog. Neurobiol. 2009;87:31–40.

[6] Wang J, Che YQ, Zhou SS, Deng B. Unidirectional synchronization of Hodgkin-Huxley neurons exposed to ELF electric field. Chaos Solit. Fract. 2009;39:1335–1345.

[7] Gerodimos NA, Daltzis PA, Hanias MP, Nistazakis HE, Tombras GS. Unimodal 1-D maps cousins in nature. New research trends in nonlinear circuits: design, chaotic phenomena and applications. ISBN: 978–1–3321–406–4, New York: Nova Publishers; 2014.

[8] Liu X, Chen T. Synchronization of identical neural networks and other systems with an adaptive coupling strength. Int. J. Circ. Theor. Appl. 2010;38:631–648.

[9] Hanias MP, Nistazakis HE, Tombras GS. Optoelectronic chaotic circuits. Optoelectronic devices and properties. Croatia: Intech Publishers; 2013. ISBN: 978–953–307–204–3.

[10] Jafari S, Haeri M, Tavazoei MS. Experimental study of a chaos-based communication system in the presence of unknown transmission delay. Int. J. Circ. Theor. Appl. 2010;38:1013–1025.

[11] Dimitriev AS, Kletsovi AV, Laktushkin AM, Panas AI, Starkov SO. Ultrawideband wireless communications based on dynamic chaos. J. Commun. Technol. Electron. 2006;51:1126–1140.

[12] Grassi G, Mascolo S. Synchronization of high-order oscillators by observer design with application to hyperchaos-based cryptography. Int. J. Circ. Theor. Appl. 1999;27:543–553.

[13] Volos CK, Kyprianidis, IM, Stouboulos IN. Experimental demonstration of a chaotic cryptographic scheme. WSEAS Trans. Circ. Syst. 2006;5:1654–1661.

[14] Luo ACJ, editor. Dynamical system synchronization. New York: Springer; 2013. 239 p.

[15] Fujisaka H, Yamada T. Stability theory of synchronized motion in coupled-oscillator systems. Prog. Theor. Phys. 1983;69:32–47.

[16] Pikovsky AS. On the interaction of strange attractors. Z. Phys. B: Condensed Matter. 1984;55:149–154.

[17] Pecora LM, Carroll TL. Synchronization in chaotic systems. Phys. Rev. Lett. 1990;64:521–524.

[18] Maritan A, Banavar J. Chaos noise and synchronization. Phys. Rev. Lett. 1994;72:1451–1454.

[19] Kyprianidis IM, Stouboulos IN. Synchronization of two resistively coupled nonautonomous and hyperchaotic oscillators. Chaos Solit. Fract. 2003;17:314–325.

[20] Kyprianidis IM, Stouboulos IN. Synchronization of three coupled oscillators with ring connection. Chaos Solit. Fract. 2003;17:327–336.

[21] Woafo P, Enjieu Kadji HG. Synchronized states in a ring of mutually coupled self-sustained electrical oscillators. Phys. Rev. E. 2004;69:046206.

[22] Kyprianidis IM, Volos CK, Stouboulos IN, Hadjidemetriou J. Dynamics of two resistively coupled Duffing-type electrical oscillators. Int. J. Bifurcat. Chaos. 2006;16:1765–1775.

[23] Kyprianidis IM, Volos CK, Stouboulos IN. Experimental synchronization of two resistively coupled Duffing-type circuits. Nonlin. Phenom. Complex Syst. 2008;11:187–192.

[24] Dykman GI, Landa PS, Neymark YI. Synchronizing the chaotic oscillations by external force. Chaos Solit. Fract. 1991;1:339–353.

[25] Parlitz U, Junge L, Lauterborn W, Kocarev L. Experimental observation of phase synchronization. Phys. Rev. E. 1996;54:2115–2217.

[26] Rosenblum MG, Pikovsky AS, Kurths J. From phase to lag synchronization in coupled chaotic oscillators. Phys. Rev. Lett. 1997;78:4193–4196.

[27] Taherion S, Lai YC. Observability of lag synchronization of coupled chaotic oscillators. Phys. Rev. E. 1999;59:R6247–R6250.

[28] Rulkov NF, Sushchik MM, Tsimring LS, Abarbanel HDI. Generalized synchronization of chaos in directionally coupled chaotic systems. Phys. Rev. E. 1995;51:980–994.

[29] Kim CM, Rim S, Kye WH, Rye JW, Park YJ. Anti-synchronization of chaotic oscillators. Phys. Lett. A. 2003;320:39–46.

[30] Liu W, Qian X, Yang J, Xiao J. Antisynchronization in coupled chaotic oscillators. Phys. Lett. A. 2006;354:119–125.

[31] Cao LY, Lai YC. Antiphase synchronism in chaotic system. Phys. Rev. 1998;58:382–386.

[32] Astakhov V, Shabunin A, Anishchenko V. Antiphase synchronization in symmetrically coupled self-oscillators. Int. J. Bifurcat. Chaos. 2000;10:849–857.

[33] Zhong GQ, Man KF, Ko KT. Uncertainty in chaos synchronization. Int. J. Bifurcat. Chaos. 2001;11:1723–1735.

[34] Blazejczuk-Okolewska B, Brindley J, Czolczynski K, Kapitaniak T. Antiphase synchronization of chaos by noncontinuous coupling: two impacting oscillators. Chaos Solit. Fract. 2001;12:1823–1826.

[35] Kyprianidis IM, Bogiatzi AN, Papadopoulou M, Stouboulos IN, Bogiatzis GN, Bountis T. Synchronizing chaotic attractors of Chua's canonical circuit. The case of uncertainty in chaos synchronization. Int. J. Bifurcat. Chaos. 2006;16:1961–1976.

[36] Tsuji S, Ueta T, Kawakami H. Bifurcation analysis of current coupled BVP oscillators. Int. J. Bifurcat. Chaos. 2007;17:837–850.

[37] Mainieri R, Rehacek J. Projective synchronization in three-dimensional chaotic system. Phys. Rev. Lett. 1999;82:3042–3045.

[38] Voss HU. Anticipating chaotic synchronization. Phys. Rev. E. 2000;61:5115–5119.

[39] Li GH. Inverse lag synchronization in chaotic systems. Chaos Solit. Fract. 2009;40:1076–1080.

[40] Gonzalez-Miranda JM. Synchronization and control of chaos. London: Imperial College Press; 2004. 212 p.

[41] Zhan M, Hu G, Yang J. Synchronization of chaos in coupled systems. Phys. Rev. E. 2000;62:2963–2966.

[42] Wang J, Che YQ, Zhou SS, Deng B. Unidirectional synchronization of Hodgkin-Huxley neurons exposed to ELF electric field. Chaos Solit. Fract. 2009;39:1335–1345.

[43] Tass P, Rosemblum MG, Weule MG, Kurths J, Pikovsky A, Volkmann J, Schnitzler A, Freund HJ. Detection of *n*:*m* phase locking from noise data: Application to magneto-encephalography. Phys. Rev. Lett. 1998;81:3291–3294.

[44] Tognoli E, Kelso JAS. Brain coordination dynamics: True and false faces of phase synchrony and metastability. Prog. Neurobiol. 2009;87:31–40.

[45] Shaw R. Strange attractors, chaotic behavior, and information flow. Z. Nat. 1981;361:80–112.

[46] Hasselblatt B, Katok A. A first course in dynamics: with a panorama of recent developments. Cambridge: University Press; 2003. 419 p.

[47] Tacha OI, Volos ChK, Kyprianidis IM, Stouboulos IN, Vaidyanathan S, Pham V-T. Analysis, adaptive control and circuit simulation of a novel nonlinear finance system. Appl Math Comput. 2016;276:200–217.

[48] Manneville P, Pomeau Y. Intermittency and the Lorenz model. Phys Lett. 1979;75A:1–2.

[49] Grebogi C, Ott E, Yorke JA. Crises, sudden changes in chaotic attractors and chaotic transients. Phys. D. 1983;7:181–200.

[50] Rollins RW, Hunt ER. Intermittent transient chaos at interior crisis in the diode resonator. Phys Rev A. 1984;29:3327.

[51] Padmanaban E, Hens C, Dana K. Engineering synchronization of chaotic oscillator using controller based coupling design. Chaos. 2011;21:013110.

[52] Volos CK, Pham V-T, Vaidyanathan S, Kyprianidis IM, Stouboulos IN. Synchronization phenomena in coupled hyperchaotic oscillators with hidden attractors using a nonlinear open loop controller. In: Advances and applications in chaotic systems. Switzerland: Springer International Publishing; 2016. p. 1–38.